Small polaron migration associated multiple dielectric responses of multiferroic DyMnO3 polycrystal in low temperature region

J. Yang, J. He, J.Y. Zhu, W. Bai, Luyan Sun, X.J. Meng, X.D. Tang, C.G. Duan, Denis Remiens, J.H. Qiu, et al.

Small polaron migration associated multiple dielectric responses of multiferroic $DyMnO_3$ polycrystal in low temperature region

Cite as: Appl. Phys. Lett. **101**, 222904 (2012); https://doi.org/10.1063/1.4768790
Submitted: 22 August 2012 • Accepted: 09 November 2012 • Published Online: 29 November 2012

J. Yang, J. He, J. Y. Zhu, et al.

Small polaron migration associated multiple dielectric responses of multiferroic $DyMnO_3$ polycrystal in low temperature region

J. Yang,[1,2,a)] J. He,[1] J. Y. Zhu,[1] W. Bai,[1] L. Sun,[1,b)] X. J. Meng,[2] X. D. Tang,[1] C.-G. Duan,[1,2] D. Rémiens,[3] J. H. Qiu,[4] and J. H. Chu[1,2]
[1]*Key Laboratory of Polar Materials and Devices, Ministry of Education, East China Normal University, Shanghai 200241, China*
[2]*National Laboratory for Infrared Physics, Shanghai Institute of Technical Physics, Chinese Academy of Science, Shanghai 200083, China*
[3]*IEMN-DOAE, CNRS, UMR 8520, University of Valenciennes, 59313 Valenciennes cedex 9, France*
[4]*Center for Low-Dimensional Materials, Micro-Nano Devices and System, Changzhou University, Changzhou 213164, China*

(Received 22 August 2012; accepted 9 November 2012; published online 29 November 2012)

Utilizing temperature dependent dielectric/impedance spectroscopy, multi-dielectric responses involving two dielectric relaxations (DRs) and two magnetic-order-associated dielectric anomalies were observed in polycrystalline $DyMnO_3$. It is elucidated that both DRs' dynamics, established in terms of equivalent circuit model and small polaron (SP) theories, are closely linked with localized SP migration features. Namely, low-temperature relaxation process can be attributed to short range polaronic variable-range-hopping induced dipolar-type relaxation in grains, whereas the higher-temperature one is due to Maxwell-Wagner relaxation at grain/grain boundary interfaces, which are governed by SP nearest-neighbor-hopping conduction. Additionally, magnetic-orders-associated dielectric anomalies may be assigned to strong spin-lattice couplings by magnetoelasticity-aroused lattice deformation. © *2012 American Institute of Physics*. [http://dx.doi.org/10.1063/1.4768790]

Multiferroics have currently attracted considerable scientific interests for the prospect of magnetoelectric (ME) effects, fuelled by both the underlying new fundamental physics and the potential technological applications in magnetic sensors, multi-state memories, etc.[1] Recently, in virtue of a special frustrated spin structure-driven spontaneous polarization, a new category of orthorhombically distorted perovskite rare-earth manganites $REMnO_3$ (RE = Tb, Dy) was found to possess gigantic and intrinsic ME couplings.[2–14] This $REMnO_3$ system yields not only $GdFeO_3$-type but also cooperative Jahn-Teller (JT)-type distortions companied by staggered orbital order. In $REMnO_3$, the competitions between nearest-neighbor ferromagnetic (FM) and next-nearest-neighbor antiferromagnetic (AFM) exchange interactions in Mn sublattices lead to Mn^{3+} *3d* spin frustration. Thereby, noncollinear Mn transverse-spiral or cycloidal spin orders could appear.[2–6] It is generally believed that this peculiar sinusoidal AFM order breaks time-reversal and inversion symmetry simultaneously and in turn generates ferroelectric (FE) polarization via inverse Dzyaloshinski-Moriya interaction,[7] magnetoelasticity induced lattice modulation,[2] or spin current scenario.[8] More observed ME coupling evidences, such as the magnetic-field-induced FE polarization flop and electric control of spin helicity,[2,9] further reveal the magnetically activated origins of electrical polarization.

Moreover, the mechanisms corresponding to gigantic magnetocapacity (MC) effects in $REMnO_3$ system were also intensively investigated.[2,3,10–12] Katsura *et al.* attributed the huge MC to softening of the electromagnons at low frequency,[10] whereas it is more and more inclined to consider dielectric relaxations (DRs) at low temperature as a key to understand MC phenomena in $REMnO_3$.[11,12] It is suggested that the low temperature DRs possibly arise from local motion of multiferroic domain wall,[11] migration of localized charge carries,[3] or off-center motion of Mn ions.[12] However, the above studies of DRs were mainly focused on single-crystal samples. Concerning microstructural and electric inhomogeneities, dielectric response of readily achieved polycrystalline ceramics is a rather more challenging open issue. Although there are few investigations about the DRs of the $TbMnO_3$ and $DyMn_{1-x}Fe_xO_3$ polycrystals, the reported relaxation behaviors were mainly concentrated in the fairly high temperature (>100 K).[13] Because of rich physical phenomena at low temperature, such as the transitions of magnetic orders and complex competitions of various interactions in strongly correlated electronic system, it is of considerable interest to extend the studies of dielectric responses to lower temperature region. On the other hand, these strong interactions in $REMnO_3$, especially the coupling of Jahn-Teller phonons and e_g electrons, could make the carriers localized and even generate related polarons. So far the transport mechanisms of localized charge carriers in $REMnO_3$ have not yet been established. Thus, systematic investigation on these issues would elucidate physical pictures correlating dielectric responses with electrical transport of localized charged carriers, complex strongly correlated interactions, and frustrated spin order. More importantly, it will provide new insights to reveal the nature of gigantic ME/MC effects.

In this study, we present the temperature dependent dielectric/impedance spectroscopy of polycrystalline $DyMnO_3$

a)Electronic mail: jyang@ee.ecnu.edu.cn.
b)Electronic mail: lsun@ee.ecnu.edu.cn.

(DMO). A careful quantitative analysis on multiple dielectric relaxations and localized charge carrier migration behaviors over a broad temperature range was performed. Moreover, two well-defined dielectric anomalies corresponding to the spin-lattice coupling were also addressed.

DMO polycrystalline samples were synthesized by the conventional solid-state reaction method in atmosphere. The powders, mixed in stoichiometric compositions of high-purity Dy_2O_3 (99.9%, Strem) and Mn_2O_3 (99%, Aldrich), were ball-milled in ethanol for 30 h. The dried powders were pressed into pellets and then pre-sintered at 1000 °C for 6 h. The calcined pellets were ground and ball-milled in ethanol for 30 h, dried, palletized again, and finally were sintered at 1250 °C for 6 h. The relative density of the obtained DMO ceramics is about 93% using Archimedes method. The x-ray diffraction result indicates that the present sample has single orthorhombic perovskite structure with good crystallinity. After silver paste was deposited on polished sample surfaces as electrodes, the temperature variation in dielectric properties as the function of frequency was performed using an Agilent E4980A LCR meter combined with a physical property measurement system (PPMS-9, Quantum Design, USA) from 2 to 300 K.

Figure 1 shows the temperature dependent dielectric properties of DMO ceramic at several typical frequencies, from which four dielectric anomalies are observed distinctly. As the insets of Figs. 1(a) and 1(b) illustrated, the first two anomalies happen at T_{Dy} (~8 K) and T_{SSO} (~18 K), respectively, with the features that the real part of dielectric constant ε' and dielectric loss tanδ suffer pronounced sharp peaks and the peak sites are weak frequency dependence.

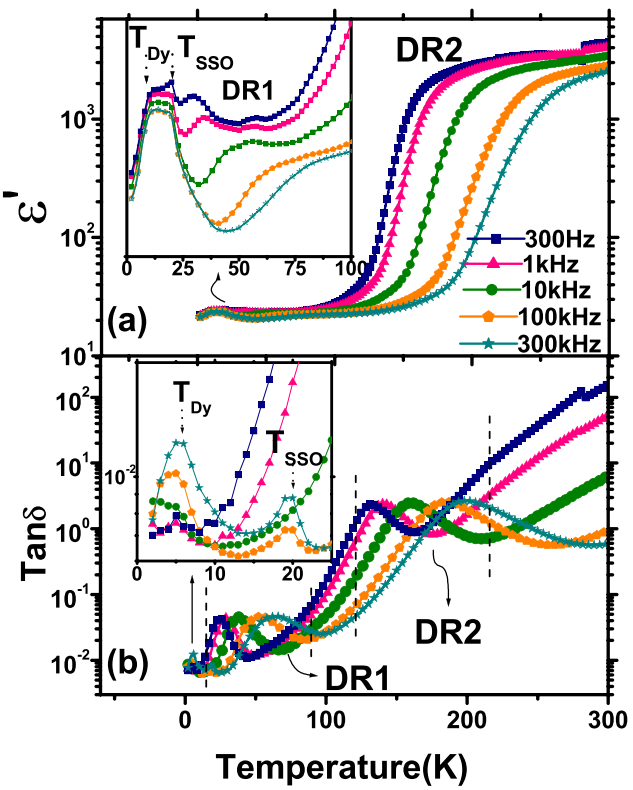

FIG. 1. Temperature dependence of (a) dielectric constant and (b) loss for DMO at various frequencies. The insets show the low temperature region on an enlarged scale.

Such anomalies also were found in thermal evolution of heat capacity and ε'(T) curves of DMO single crystals,[2,3] in which the anomalies were assigned to the strong spin-lattice couplings rooted in magnetoelasticity-induced lattice deformation.[2,3] Concretely, the anomaly at 8 K is due to the formation of Dy long range spin ordering. And the counterpart at 18 K is associated with incommensurate-commensurate (or lock in) transition, where the magnetic modulation wave vector is locked and Mn spiral spin ordering (SSO) plus Mn-Dy SSO occur.[14] It is the onset of ferroelectric polarization and the important feature of frustrated spin driven ME effect. The other two anomalies (see in Fig. 1) emerge in the temperature range 20–75 K and 130–220 K, respectively. In both cases, the behaviors are dominated by a typical relaxation characteristic: ε'(T) undergoes a steplike increase towards a large plateau value at higher temperature with marked dielectric dispersion. These step-like features in ε' are accompanied by the broad relaxation peaks in loss spectrum and the peak sites shift monotonously towards higher temperature with increasing frequency, indicating a thermally activated dynamic. The present low temperature relaxation (denoted as DR1), often observed in single crystals,[3,12] is further identified in polycrystalline DMO samples here. And the higher temperature one (DR2) is also preliminarily involved in pervious investigation.[13] Possible physical mechanisms behind these dielectric relaxations are addressed as follows.

With regard to the inhomogeneous nature of polycrystals, whether the DRs come from grain (G) or grain boundary (GB) should be foremost determined. To evaluate this point, complex impedance spectra at different temperatures are present in Figs. 2(a) and 2(b). At low temperature, only a big slope straight line of an incomplete semicircular arc is observed [Fig. 2(a)], suggesting that the DR1 is corresponding to DMO grain contribution. It is consistent with common argument that the dielectric response at low temperature and high frequency is often caused by grain parts and reveals the intrinsic performance of the bulk.[15–19] As shown in Fig. 2(c), this relaxation behavior can be well fitted by empirical Cole-Cole function,[19] $\varepsilon^* = \varepsilon_\infty + (\varepsilon_s - \varepsilon_\infty)/[1 + (j\omega\tau)^{1-\alpha}]$, where ε_s and ε_∞ are the static and high-frequency dielectric constant, respectively, τ is the relaxation time, and α represents the degree of distribution of the relaxation time. Inset of Fig. 2(c) shows β ($=1-\alpha$) undergoes a peak at Néel temperature (~40 K) for AFM ordering formation,[2] displaying a magnetic modulated DR behavior. With τ from the fittings, the dynamic of relaxation is first analyzed in the Arrhenius form, $\tau = \tau_0 \exp(E_a/k_B T)$, where E_a is the activation energy required for DR and τ_0 is a pre-exponential factor. In Fig. 3(a), ln(τ) vs. $1/T$ cannot yield a line but two slopes regions with respective $E_a = 26.9 \pm 0.3$ and 18.2 ± 0.7 meV, which agree with counterpart values of DMO single crystals in Ref. 12 [28.7 ± 0.3 and 15.1 ± 0.4 meV, in Fig. 3(b)] and Ref. 3 (25 meV). It is approved again that DR1 is ascribed to intrinsic bulk contributions. Generally, the DRs in bulk mainly derive from couplings of local polar nano-regions (PNRs),[16,17] motion of domain wall,[18] charge carriers related dipole reorientation, and localized/long-range migration.[19–24] Because of thermal fluctuation and the interactions of neighbor PNRs, the relaxation kinetics arising from PNRs yields

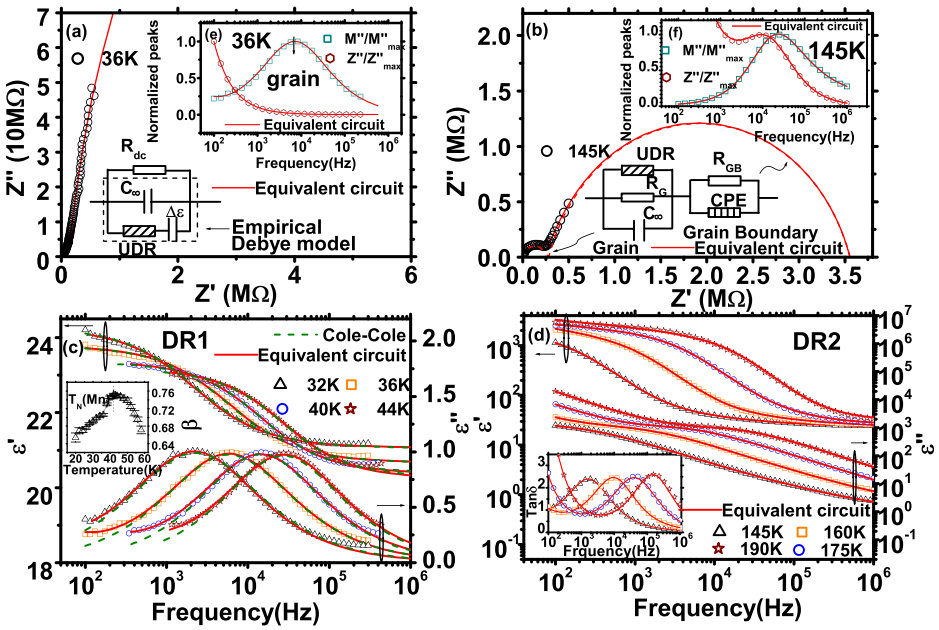

FIG. 2. Nyquist diagrams of complex-plane impedance at (a) 36 K and (b) 145 K. The insets are the equivalent circuit models corresponding to respective temperature regions. The real part and imaginary part of dielectric constant as a function of frequency for (c) DR1 and (d) DR2 at several typical temperatures. Inset of (c) is β vs. temperature relation. Inset of (d) is frequency dependent tanδ for DR2. (e) and (f) are the frequency variant of normalized impedance Z''/Z''_{max} and modulus M''/M''_{max} at 36 and 145 K, respectively.

the Vogel-Fulcher relation,[16] opposed to the present relaxation dynamics. And DR induced by the motion of domain wall often occurs at higher frequency (>1 MHz).[11] Therefore, the present DR1 possibly correlates with the migration of localized charge carriers, usually resulting in associated dipolar reorientation or fluctuation.[19]

In disorder semiconductor/insulator system, thermal assisted carrier tunneling between localized states due to spatially fluctuating potentials, namely polaronic hopping, is major migration manner at low temperature. In polaronic hopping conduction, two common hopping types are involved.[20] Arrhenius-like law ruled nearest-neighbor-hopping (NNH), Mott relations ruled variable-range-hopping (VRH). Mott relations can express the conduction and relaxation as[21] $R_{dc} = R_0 \exp[(T_0/T)^{1/4}]$, $\tau = \tau_1 \exp[(T_0/T)^{1/4}]$, where R_0, τ_1 are the constants, and $T_0 = 24/[\pi k_B N(E_F)\xi^3]$, $N(E_F)$ is the density of localized states at Fermi level, and ξ is the decay length of localized wave function. In contrast to the deviation from Arrhenius law, as Figs. 3(a) and 3(b) shown, $\ln(\tau)$ vs. $(1/T)^{1/4}$ in this case and single crystal sample (Ref. 12) follows Mott relation well at the whole temperature range, and T_0 are $(3.1 \pm 0.1) \times 10^7$ and $(2.9 \pm 0.1) \times 10^7$ K, respectively. For $\xi = 0.44$ nm, the distance between neighboring Mn ions[6] $N(E_F) \approx (3.5 \pm 0.2) \times 10^{19}\,\mathrm{eV^{-1}cm^{-3}}$. All parameters here are similar to those of $CaCu_3Ti_4O_{12}$.[21]

To further establish the correlation of the conduction and relaxation, the equivalent circuit model (ECM) including Debye model and dc conduction[19] is employed to describe DR1, which is better than Cole-Cole model alone [Figs. 2(a) and 2(c)]. The dc resistances obtained from the fittings have similar features as the relaxation kinetics, as seen in Fig. 3(c). Meanwhile, the relaxation frequency f_r keeps a linear relation with dc conduction (inset of Fig. 4), which is usually observed in polaronic relaxation systems.[21] Moreover, Fig. 2(e) indicated that the peaks of normalized impedance Z''/Z''_{max} and modulus M''/M''_{max} cannot coincide obviously, implying a short range hopping process here.[22]

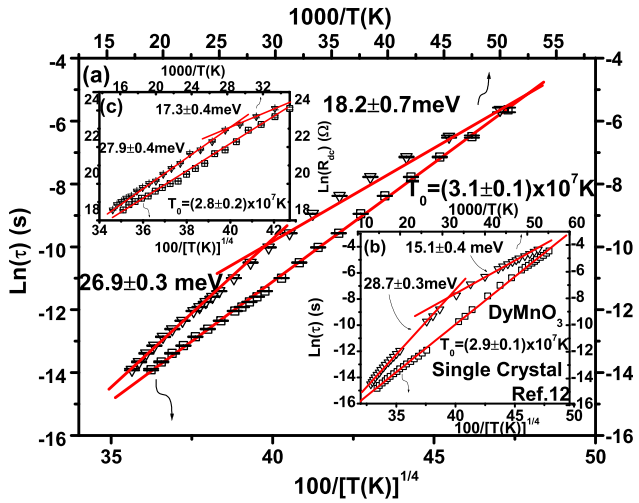

FIG. 3. Arrhenius and Mott's plots of (a) present DMO polycrystal and (b) DMO single crystal (data extracted from Ref. 12) for DR1 relaxation time. (c) Counterparts of present DMO sample for dc resistivity at low temperature.

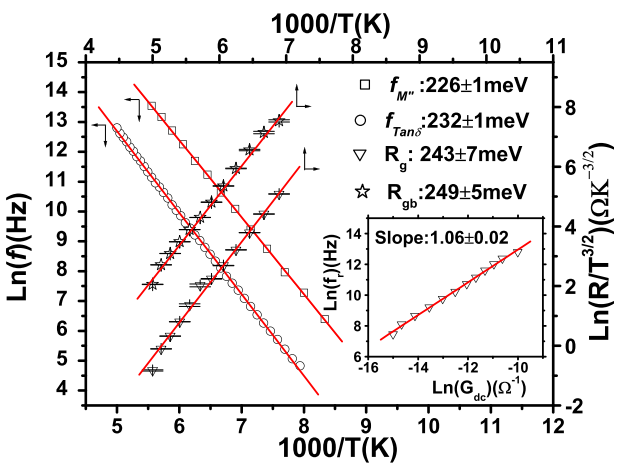

FIG. 4. Arrhenius plots of tanδ relaxation frequency, modulus relaxation frequency, grain resistivity, and grain boundary resistivity at DR2 temperature range. The latter two were obtained from the fittings of ECM. The inset is $ln(f_r)$ vs. $ln(G_{dc})$ at low temperature.

Usually, an polaron is composed of a trapped electron and its accompanying lattice distortion and often is analogous to an effective dipole made by the lattice distortion and bound electron.[19–24] Consequently, short range polaronic hopping, i.e., electron hopping with the lattice distortion, behaves like dipolar reorientation in its reciprocating motions under ac electrical field and owns similar relaxation function with an dipole.[19] Assuming electron hopping between sites occurs at a certain statistical rate, associated polarization of this equivalent dipole will have a very small phase lag with applied ac field when the frequency is much lower than the hopping rate. However, with increasing frequency, the polarization has less and less chance to keep up the field variation, and a typical dipole-like DR can be expected.[19–24] Therefore, based on the above evidences, magnetic related short range polaronic VRH induced dipolar relaxation may be reasonably interpreted as the source of DR1.

As for DR2, from Fig. 2(b), which is a typical complex impedance spectrum in DR2 region, one resolved semicircle and an inclined spike of a second semicircle were detected. This result manifests that present dielectric response could be assigned to the joint effects of G at high frequency and GB at low frequency. When ac electrical current passes through inhomogeneous G/GB interfaces, the charge carriers would be localized and accumulate at the interfaces between two media with different conductivities. This process could give rise to a so-called Maxwell-Wagner (MW) interfacial relaxation.[15,19] This MW relaxation can be evidently observed in plots of frequency dependent dielectric constant [Fig. 2(d)]. And the relaxation dynamic obeys Arrhenius relation of the relaxation frequency f_r vs. 1/T with activation energy $E_{re} \approx 0.23$ eV in Fig. 4, which is consistent with those of $TbMnO_3$ and $DyMn_{1-x}Fe_xO_3$.[13] Furthermore, DR2 was quantitatively described by ECM [inset of Fig. 2(b)],[15,19] which is in the frame of MW model and is composed of a series of two subcircuits. One is a parallel to GB resistance and constant phase element (CPE, instead of nonideal GB capacitance), the other is G resistance, capacitance, and universal dielectric response (UDR, indicative of polaron hopping conduction) in parallel. The experimental data are in good concord within this ECM, as Figs. 2(b) and 2(d) shown. Then, the resistances of G and GB were extracted by the fittings to check underlying transport mechanisms. It can be analyzed by nonadiabatic small polaron (SP) NNH type Arrhenius characteristic,[23] $R = A_0 T^{3/2} \exp(E_0/k_B T)$, $E_0 = W_H + W_D/2 + W_0/2$, where A_0 is constant, W_H, W_D, and W_0 are hopping energy, disorder energy, and generation energy of free polarons. In Fig. 4, the G and GB resistances satisfy this relation well and E_0 is estimated to be ~0.24 eV, indicating that SP NNH is the dominant conduction mechanism here. And, the peak sites of Z″ and M″ in Fig. 2(f) almost coincide, displaying a nearly long range hopping process. Note that the activation energy of MW relaxation overlaps with these of the polaron conduction. It is because that, assuming ideal two-phase system, MW relaxation time of heterostructure $\tau \approx C_{GB}R_G$, where C_{GB} and R_G are the larger capacitance and smaller resistance in two components.[15] Usually, since C_{GB} has weak temperature dependence, the relaxation dynamics is mainly determined by the thermal variant conduction transport of the grain. Consequently, it may be concluded that DR2 is SP NNH conduction governed MW relaxation. Now, the question arises: what is the origin of present SP?

Generally, the formation of the polaron is in fact a charge carrier self-localization or trapping process in energetically favorable local lattice distortion, which may result from electron-phonon (*e-p*) coupling and/or structural/compositional defects.[20,23–25] In consideration of above mentioned evidences that the present polaron is magnetic dependency in DR1, the sublattices containing Mn^{3+} ions may play a crucial role in the generation of the polarons. Most probably, as a member of orthorhombically distorted manganites, DMO also undergoes Jahn-Teller distortion, where in-plane Mn-O bonds of MnO_6 octahedrons are shorted and two others across the plane are stretched. JT distortion further splits the degenerate *3d* e_g doublet orbitals of Mn^{3+} in octahedrons.[4–6] This JT effect is responsible for the interaction of particular lattice vibrational modes (JT phonons) and orbitally degenerate e_g electronic states and finally localizes e_g electrons in splitting levels. Strong coupling of localized e_g to JT lattice distortion may cause the SP, termed JT polaron.[26] Here, NNH energy lies in ~0.23 eV, in good agreement with those of JT polaron in $La_xR_{1-x}MnO_3$ systems (0.2–0.3 eV).[27] We noted that DR1 only occurs along the c-axis in single crystal.[3] It is because that the JT distortion generally possesses a typical anisotropic nature,[28] which may lead to anisotropic electron-lattice interaction and therefore anisotropic polaron effects.[29] Moreover, complex anisotropic interactions of orbital and spin orders in manganites may also account for anisotropic electron hopping and related polaronic relaxation.[30] Hence, JT polaron may be the main origin of SP here. Otherwise, because of inevitable existence of the oxygen vacancies in the oxides, heterovalent Mn ions can be expected to keep electrical neutral of the system. The carriers hopping between heterovalent Mn with different ionic radii may induce lattice deformation and thus also may lead to SPs.[13,25]

The evolution of hopping mechanism in this case is also found to be accorded with the classic small polaron hopping theory.[20] Namely, at high temperature, optical multiphonon processes provide SP sufficient energy to excite the hopping between nearest-neighbor localized states, where $E_{re} = W_H + W_D/2$. However, with the further decrease of temperature, where the carriers are in more localized Anderson states, a single acoustical phonon assisted tunneling Mott VRH conduction takes over frozen NNH. This type of hopping occurs in small region ($\sim k_B T$) near Fermi energy with various hopping length for each hop because thermal fluctuation energy is insufficient to excite the carriers across the nearest-neighbor Coulomb gap but tunneling to non-spatially associated localized states closest to Fermi level, and $E_{re} = W_D$ (~27 meV). According to the above obtained activation energy, W_H is about ~0.22 eV here. This polaron hopping energy can be evaluated by Austin and Mott's relation,[20] $W_H = e^2(1/r_p - 1/R)(1/\varepsilon_\infty - 1/\varepsilon_{static})/4$ (in C. G. S units), where R is Mn-O-Mn distance along c-axis (4.4 Å),[6] the polaron radius $r_p = 0.5\,R(\pi/6)^{1/3}$, ε_∞ (~4) and ε_{static}(~30) are the high frequency and static dielectric constants. Then $r_p = 1.77$ Å within comparable size of a cell lattice scale and W_H is calculated to be about 0.26 eV, just a little larger than

experimental value, which further confirming the existence of SPs. Moreover, the strength *e-p* interaction can be estimated from the polaron binding energy $W_p \approx 2W_H = \gamma\hbar\omega_{ph}$,[20] where ω_{ph} is optical phonon frequency (usually ~600 cm^{-1} for optical Mn-O vibration in magnates[26,27]) γ, polaron coupling constant, is calculated to be ~5.5, similar to that of $La_xSr_{1-x}MnO_3$ (~7.5)[26], implying a strong *e-p* interaction in DMO system ($\gamma > 4$). Finally, according to Sewell polaron model,[31] the effective mass of polaron (m_p) is calculated to be about 9.5 m_e,[32] which is within order of magnitude of the counterparts obtained from Seebeck and Hall effects (4–20 m_e).[31]

The work was supported by "973" Program(2013CB922300), Natural Science Foundation of China (Grant Nos. 11104074, 61176011, 10904053, 61076060, and 50832003), Natural Science Foundation of Shanghai (Nos. 11ZR1410800 and 10DJ1400201) and Jiangsu (09KJB140002), Fundamental Research Funds for the Central Universities (ECNU), and PCSIRT.

[1]J. F. Scott, Science **315**, 954 (2007); N. A. Spaldin and M. Fiebig, *ibid.* **309**, 391 (2005); W. Eerensein *et al*., Nature **442**, 759 (2006); K. F. Wang, J.-M. Liu, and Z. F. Ren, Adv. Phys. **58**, 321 (2009).
[2]T. Kimura, T. Goto, H. Shintani, K. Ishizaka, T. Arima, and Y. Tokura, Nature **426**, 55 (2003).
[3]T. Goto, T. Kimura, G. Lawes, A. P. Ramirez, and Y. Tokura, Phys. Rev. Lett. **92**, 257201 (2004).
[4]T. Kimura, S. Ishihara, H. Shintani, T. Arima, K. T. Takahashi, K. Ishizaka, and Y. Tokura, Phys. Rev. B **68**, 060403(R) (2003).
[5]F.-K. Chiang, M.-W. Chu, F. C. Chou, H. T. Jeng, H. S. Sheu, F. R. Chen, and C. H. Chen, Phys. Rev. B **83**, 245105 (2011).
[6]J. M. Chen, Z. Hu, H. T. Jeng, Y. Y. Chin, J. M. Lee, S. W. Huang, K. T. Lu, C. K. Chen, S. C. Haw, T. L. Chou *et al*., Phys. Rev. B **81**, 201102(R) (2010).
[7]I. A. Sergienko and E. Dagotto, Phys. Rev. B **73**, 094434 (2006).
[8]H. Katsura, N. Nagaosa, and A. V. Balatsky, Phys. Rev. Lett. **95**, 057205 (2005).
[9]Y. Yamasaki, H. Sagayama, T. Goto, M. Matsuura, K. Hirota, T. Arima, and Y. Tokura, Phys. Rev. Lett. **98**, 147204 (2007).
[10]H. Katsura, A. V. Balatsky, and N. Nagaosa, Phys. Rev. Lett. **98**, 027203 (2007).
[11]F. Kagawa, M. Mochizuki, Y. Onose, H. Murakawa, Y. Kaneko, N. Furukawa, and Y. Tokura, Phys. Rev. Lett. **102**, 057604 (2009); F. Kagawa, Y. Onose, Y. Kaneko, and Y. Tokura, Phys. Rev. B **83**, 054413 (2011).
[12]F. Schrettle, P. Lunkenheimer, J. Hemberger, V. Yu. Ivanov, A. A. Mukhin, A. M. Balbashov, and A. Loidl, Phys. Rev. Lett. **102**, 207208 (2009).
[13]C. C. Wang, Y. M. Cui, and L. W. Zhang, Appl. Phys. Lett. **90**, 012904 (2007); F. Hong, Z. X. Cheng, S. J. Zhang, and X. L. Wang, J. Appl. Phys. **111**, 034104 (2012).
[14]N. Zhang, Y. Y. Guo, L. Lin, S. Dong, Z. B. Yan, X. G. Li, and J.-M. Liu, Appl. Phys. Lett. **99**, 102509 (2011).
[15]P. Lunkenheimer, S. Krohns, S. Riegg, S. G. Ebbinghaus, A. Reller, and A. Loidl, Eur. Phys. J. Spec. Top. **180**, 61 (2010).
[16]D. Viehland, S. J. Jang, L. E. Cross, and M. Wuttig, J. Appl. Phys. **68**, 2916 (1990).
[17]G. A. Samara, J. Phys.: Condens. Matter **15**, R367 (2003).
[18]V. P. Bovtoun and M. A. Leshchenko, Ferroelectric **190**, 185 (1997).
[19]A. K. Jonscher, *Dielectric Relaxation in Solids* (Chelsea Dielectrics, London, 1983); J. R. Macdonald, *Impedance Spectroscopy* (John Wiley, New York, 1987).
[20]K. K. Som and B. K. Chaudhuri, Phys. Rev. B **41**, 1581 (1990); I. G. Austin and N. F. Mott, Adv. Phys. **18**, 41 (1969).
[21]L. Zhang and Z. J. Tang, Phys. Rev. B **70**, 174306 (2004).
[22]D. K. Pradhan, R. N. P. Choudhary, C. Rinaldi, and R. S. Katiyar, J. Appl. Phys. **106**, 024102 (2009); A. Chen, Y. Zhi, and L. E. Cross, Phys. Rev. B **62**, 228 (2000).
[23]E. Iguchi, N. Kubota, T. Nakamori, N. Yamamoto, and K. J. Lee, Phys. Rev. B **43**, 8646 (1991).
[24]O. Bidault, M. Maglione, M. Actis, M. Kchikech, and B. Salce, Phys. Rev. B **52**, 4191 (1995).
[25]P. R. Bueno, R. Tararan, R. Parra, E. Joanni, M. A. Ramırez, W. C. Ribeiro, E. Longo, and J. A. Varela, J. Phys. D: Appl. Phys. **42**, 055404 (2009).
[26]A. Shengelaya, G. M. Zhao, H. Keller, and K. A. Müller, Phys. Rev. Lett. **77**, 5296 (1996); P. Mandal, B. Bandyopadhyay, and B. Ghosh, Phys. Rev. B. **64**, 180405(R) (2001).
[27]J. M. De Teresa, K. Dörr, K. H. Müller, L. Schultz, and R. I. Chakalova, Phys. Rev. B **58**, 5928(R) (1998); K. P. Neupane, J. L. Cohn, H. Terashita, and J. J. Neumeier, Phys. Rev. B **74**, 144428 (2006).
[28]M. K. Srivastava, A. Kaur, and H. K. Singh, Appl. Phys. Lett. **100**, 222408 (2012).
[29]P. E. Kornilovitch, Phys. Rev. B **59**, 13531 (1999).
[30]Y. Tokura and N. Nagaosa, Science **288**, 462 (2000).
[31]G. L. Sewell, Philos. Mag. **3**, 1361 (1958); E. Yagi, R. R. Hasiguti, and M. Aono, Phys. Rev. B **54**, 7945 (1996); H. Muta, T. Kanemitsu, K. Kurosaki, and S. Yamanaka, J. Alloys Compd. **469**, 50 (2009).
[32]In Ref. 31, when $T < \hbar\omega_{ph}/2k_B$ (429 K here), the polaron effective mass is $m_p = m^*\exp(S/n^2)$, where $m^* = \hbar^2/2JR^2$ is the rigid-lattice effective mass of the electron, $J \sim e^3\ [N(E_F)/\varepsilon^3{}_\infty]$, S is nearly temperature independent and approximated by $S\ (T=0) = 16Z^2e^4/3\hbar M\omega^3{}_{ph}b^4$, Z (~3) is the charge of a positive ion, M is the reduced ion mass (~2×10^{-26} kg), b is lattice distance (7.3 Å c-axis), n is optical constant (~2). Then, $m_p \approx 9.5\ m_e$.